HEFAT2007
5th International Conference on Heat Transfer, Fluid Mechanics and Thermodynamics
Sun City, South Africa
MR3

AN EXPERIMENTAL STUDY OF A PLUNGING AIRFOIL IN THE POST STALL REGION

Rasi Marzabadi F.* and Soltani M.R.
Department of Aerospace Engineering,
Sharif University of Technology,
Tehran, 11365-8639,
Iran,
E-mail: faeezehrasi@gmail.com

ABSTRACT

A series of low speed wind tunnel tests were conducted to study the unsteady flow events on an airfoil oscillating in plunge mode beyond its static-stall angle of attack. Data were acquired at a Reynolds number of $0.42*10^6$, over a range of reduced frequencies, k=0.03-0.1 and plunging amplitude of ±15cm. It was found that in the post stall region, there existed a fully separated flow over the upper surface of the airfoil and the dynamic stall vortex formed in the vicinity of the leading edge region. Also, the effect of the reduced frequency was investigated.

INTRODUCTION

Unsteady separated flows occur frequently on oscillating airfoils which have practical applications to helicopter blades, aircraft manoeuvrability, wind turbines, and jet engine compressor blades. If thoroughly understood and properly controlled, unsteady separated flows could be reduced significantly or even harnessed, thereby dramatically enhancing performance for a broad spectrum of fluid dynamic systems [1-3].

One unsteady, nonlinear aerodynamic problem of particular significance on wind turbines is dynamic stall. This is a transient stall effect that can result in unsteady aerodynamic forces being produced and are considerably in excess of what would be expected or predicted under steady conditions. Dynamic stall phenomenon has been extensively studied experimentally, mostly using oscillating two-dimensional airfoils in wind tunnels [4-7]. The majority of the documented experimental results are for airfoils oscillating in pitch. There exist limited amounts of data available for another type of motions, such as plunging oscillation. Different modes of forcing are very desirable in the study of dynamic stall because the problem may contain nonlinear physics of great importance that cannot be understood by examining the airfoil behaviour in response to only one type of motion. Most of the angle of attack changes that the rotor blades encounter are in fact due to the variations in flapping and elastic bending of the blade, i.e., a plunging type forcing. Plunging experiments are useful because pitch rate effects can be isolated from the problem [8].

This study addresses some of the most important aspects of the unsteady aerodynamic behaviour of an airfoil oscillating in plunge mode with two different mean angles of attack; 13º and 18º, beyond the static-stall angle of attack of the model (about 10º). The airfoil used in this study is a section of a 660 kW wind turbine blade under construction.

NOMENCLATURE

α_0	[deg]	mean angle of attack
C_P	[-]	pressure coefficient
c	[m]	airfoil chord
h	[m]	plunging displacement
H	[m]	amplitude of oscillation
x	[m]	distance from the leading edge of the airfoil
f	[Hz]	oscillation frequency
T	[s]	Period of oscillation
U_∞	[m/s]	freestream velocity
k	[rad]	reduced frequency, $k=\pi fc/U_\infty$
τ	[-]	Dimensionless time, $\tau=t/T$
ω	[rad/s]	Angular velocity

EXPERIMENTAL APPARATUS

The experiments were conducted in a low speed wind tunnel in Iran. It is a closed circuit tunnel with a rectangular test section of 80*80*200 cm^3. The test section speed varies continuously from 10 to 100 m/s. The model considered in the present study has 25cm chord and 80cm span. This airfoil is equipped with 64 pressure orifices on its upper and lower

surfaces. The pressure ports are located along the chord at an angle of 20 degrees with respect to the model span to minimize disturbances from the upstream taps, Fig. 1. Data were obtained using sensitive pressure transducers. Due to high number of pressure ports and the size of the selected pressure transducers, it wasn't possible to place the transducers inside the model. Therefore, extensive experiments were conducted to ensure that the time takes for the pressure to reach the transducers is much less than the frequency response of the transducers themselves, nominally 1 msec [9]. Finally the tube length and the material that gave minimum time lag for all applied pressures were selected. Each transducer data is collected via a terminal board and transformed to the computer through a 64 channel, 12-bit Analogue-to-Digital (A/D) board capable of an acquisition rate of up to 500 kHz.

The oscillation system uses a crankshaft to convert the circular motion of the motor to a reciprocal motion, which is transferred to the model by means of a rod. The oscillation amplitude was varied sinusoidally as $h = \bar{h}\sin(\omega t)$. The system can oscillate the model with frequencies ranging from 1 to 4 Hz, Fig. 2.

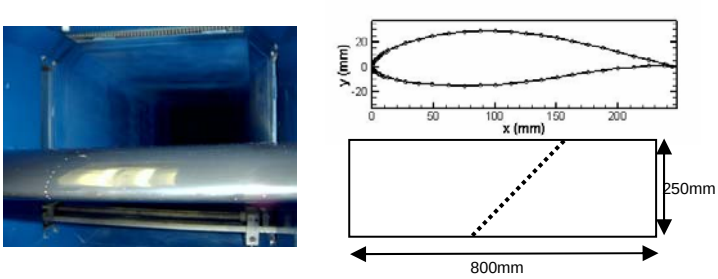

Figure 1 Airfoil model and the location of the pressure ports

Figure 2 Plunging oscillation system

RESULTS AND DISCUSSION

The airfoil surface pressure distribution was measured at a constant freestream velocity of 30m/s, with mean angles of attack of 13º and 18º, over a range of reduced frequencies, k=0.03-0.1 and at a plunging amplitude of ±15cm.

In figures 3 and 4, the data are shown for pressure ports located at x/c=0.5%, 2%, 5%, 15% and 30% of the upper surface and 15% of the lower surface. Furthermore, a drawing of the model with location of the pressure ports under study is shown in each figure. The effect of reduced frequency on the surface pressure variations is shown inside the figure, too. From Fig. 3, it is seen that for the case of α_0=13º, a hysteresis loop in the pressure signature exists and the direction of the loops are clockwise for all pressure ports of the upper surface. It means that the dynamic pressure data in the downstroke portion of the motion lead their corresponding one during the upstroke one (Note that the positive of plunging displacement is considered downstroke). However, for the upper surface pressure port located after x/c=15%, Fig. 3d, the variations of C_P is very small, almost a straight line. This indicates that oscillation of the airfoil has no significant effect on the rear portion, adverse pressure gradient region of the model. For the lower surface the direction of the loops is counterclockwise, Fig. 3f. By inspecting Fig. 3, it is seen that increasing the reduced frequency has a pronounced effect on the surface pressure in the vicinity of the leading edge, x/c≤5%. For these pressure ports, as the reduced frequency is increased from k=0.03 to k=0.06, the hysteresis loop widens, hence varying the corresponding aerodynamic parameters.

Figure 4 shows that by plunging the airfoil at higher mean incident angles, the maximum suction, $|C_{Pmax}|$, increases. The direction of hysteresis loops for the upper surface signatures change from clockwise to counterclockwise for pressure ports located at x/c=5% and beyond. It means that due to the existence of the separated flow after this port, the variations of the surface pressure in the upstroke and downstroke motions changes. It is also seen that only in the vicinity of the leading edge, x/c≤2%, increasing the reduced frequency widens the hysteresis loop of the surface pressure.

For oscillating with mean angle of attack of 18º, a "carpet" like graph of C_P is shown in Fig. 5a. It is evident that after the maximum suction, very close to the leading edge, a sudden drop in $|C_P|$ occurs which may indicate the presence of the dynamic vortex shedding from the leading edge of the model. Figures 5b-d show the variations of the dynamic pressure coefficient with dimensionless time for 7 upper surface pressure ports in the leading edge region (from leading edge to x/c=2%), for three different reduced frequencies, k=0.03, 0.045 and 0.06. These figures are parts of Fig. 5a; however, the phenomenon under study is more visible by these figures. The surface pressure shows a slight suction peak (marked with circle in Figs. 5b-d), indicating the start of vortex formation by the boundary layer separation. Successive peak at pressure port locating aft of the leading edge shows that the vortex passes the airfoil leading edge and moves back and forth, however, it does not leave the surface of the model. By increasing the reduced frequency the speed of the vortex movement on the surface increases, too. It is detected from fewer suction peaks for higher reduced frequency cases in one cycle oscillation and also from sharper slope of successive peaks at pressure ports locating aft of the leading edge.

Dynamic stall characteristics are caused by two viscous flow effects at moderate amplitudes and frequencies. One is the

integrated effect of the time-lagged external pressure gradient on the boundary layer development. The other is the so-called "leading-edge jet" effect. As the airfoil leading edge moves upward, the boundary layer between the stagnation and separation points experiences a moving wall/wall jet effect very similar to that observed on a rotating cylinder. Thus the dynamic boundary layer has a fuller profile than the steady case and, therefore, resists the adverse pressure gradient more, hence delaying separation phenomenon. On the downstroke, the effect is opposite, and the separation is promoted. There is an additional viscous flow effect of the spilled leading-edge vortex at larger amplitudes and higher frequencies [3].

Figure 6 shows the carpet-like graph and the corresponding variations of the C_P in the leading edge region, for α_0=13º at reduced frequency of 0.045. In contrast to the cases of α_0=18º, there is no indication of suction peak and vortex passage in the vicinity of the leading edge region. It means that the dynamic stall vortex has not formed, yet and the separation from the leading edge has not occurred.

CONCLUSION

An extensive experimental investigation was conducted to study the unsteady flow events on an airfoil oscillating in plunge mode beyond its static-stall angle of attack. It was found that by oscillating the airfoil in the post stall region, a fully separated flow region formed over the upper surface, however, the maximum suction increased and its location moved toward the leading edge. Variation of $|C_P|$ during the entire dynamic motion was very strong. The effect of reduced frequency was to increase the suction on the upper surface of the airfoil. It was seen that the dynamic stall vortex formed in the vicinity of the leading edge region, but did not move over the entire airfoil chord, since the range of angle of attack variation was small.

REFERENCES

[1] Lee, T. and Basu, S. Measurement of unsteady boundary layer developed on an oscillating airfoil using multiple hot-film sensors, *Experiments in Fluids,* 25 (1998), 108-117.

[2] Carta, F. A., A Comparison of the Pitching and Plunging Response of an Oscillating Airfoil, *NASA CR-3172*, 1979.

[3] Ericson, L.E., and Reding, J.P., Unsteady Flow Concepts for Dynamic stall Analysis, *AIAA Journal of Aircraft,* Vol.21, No. 8, 1984, pp. 601-606.

[4] McAlister, K.W., Carr, L.W., and McCroskey, W.J., Dynamic Stall Experiments on the NACA 0012 Airfoil, *NASA TP-1100,* January 1978.

[5] Ericsson, L.E., and Reding, J.P., Shock-Induced Dynamic Stall, *Journal of Aircraft,* Vol. 21, May 1984, pp. 316-321.

[6] Carr, L.W., Progress in Analysis and Prediction of Dynamic Stall, *AIAA Journal*, Vol. 25, No. 1, 1988, pp. 6-17.

[7] Fukushima, T. and Dadone, L.U., Comparison of Dynamic Stall Phenomena for Pitching and Vertical Translation Motions, *NASA CR-2793,* July 1977.

[8] Tayler, Joseph C., and Leishman, J. Gordon, An A.nalysis of Pitch and Plunge Effects on Unsteady Airfoil Behavior, *Presented at the 47th Annual Forum of the American Helicopter Society,* May1991.

[9] Soltani, M.R., Rasi, F., Seddighi, M., and Bakhshalipour, A., An Experimental Investigation of Time Lag in Pressure-Measuring Systems, *AIAC-2005-028, presented at 2nd Ankara International Aerospace Conference,* 2005.

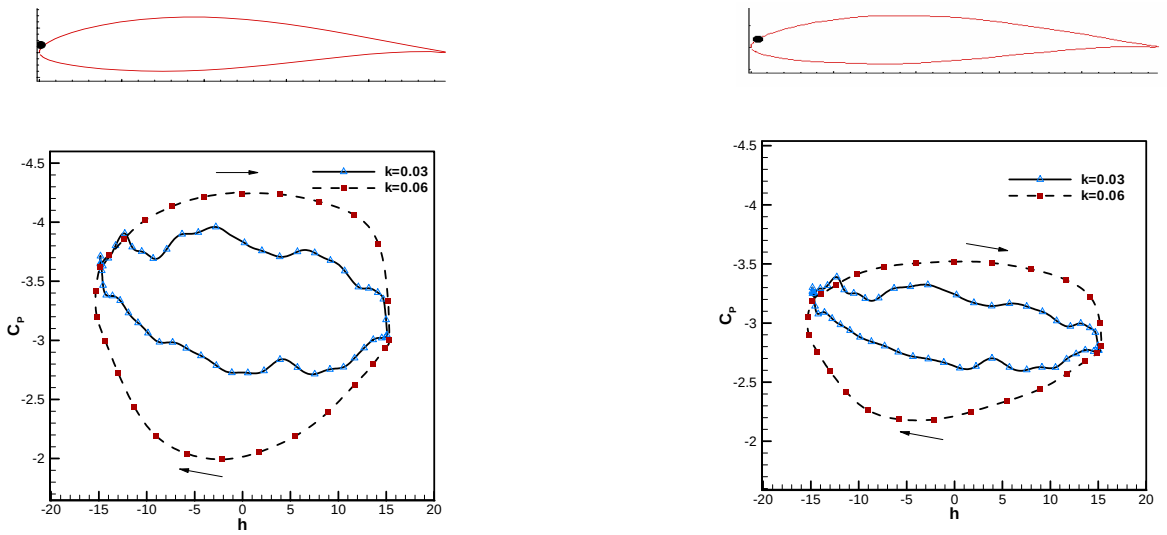

a) x/c=0.5% Upper Surface

b) x/c=2% Upper Surface

c) x/c=5% Upper Surface

d) x/c=15% Upper Surface

e) x/c=30% Upper Surface

f) x/c=30% Lower Surface

Figure 3 Variations of the pressure coefficient with h, α_0=13°

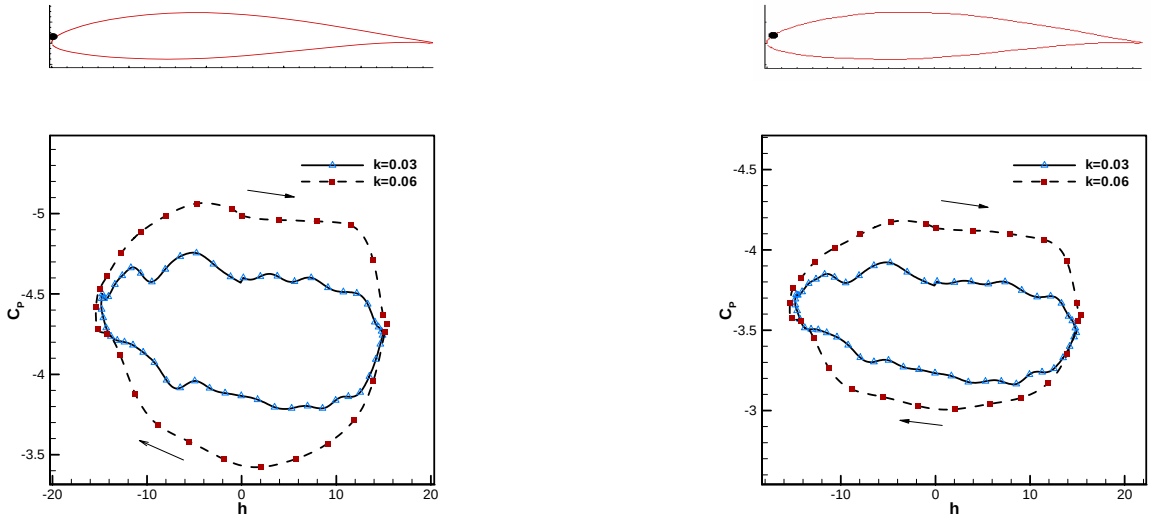

a) x/c=0.5% Upper Surface

b) x/c=2% Upper Surface

c) x/c=5% Upper Surface

d) x/c=15% Upper Surface

e) x/c=30% Upper Surface

f) x/c=30% Lower Surface

Figure 4 Variations of the pressure coefficient with h, α_0=18º

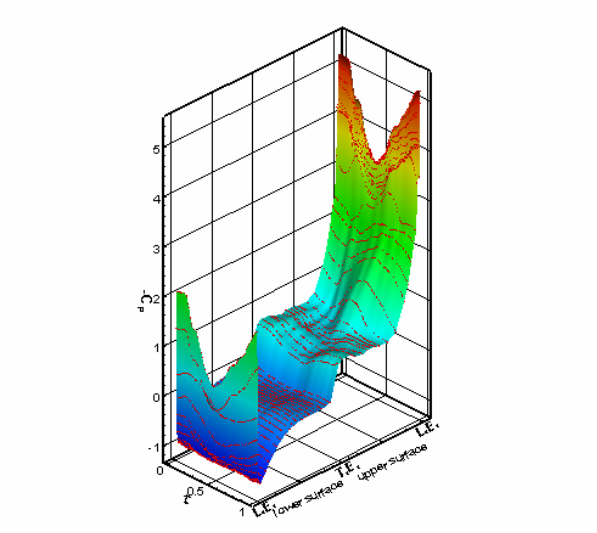

a) carpet-like graph of C_P, k=0.06

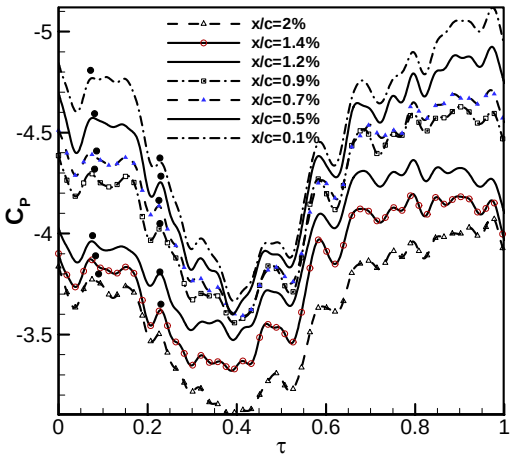

b) upper surface, near leading edge, k=0.03

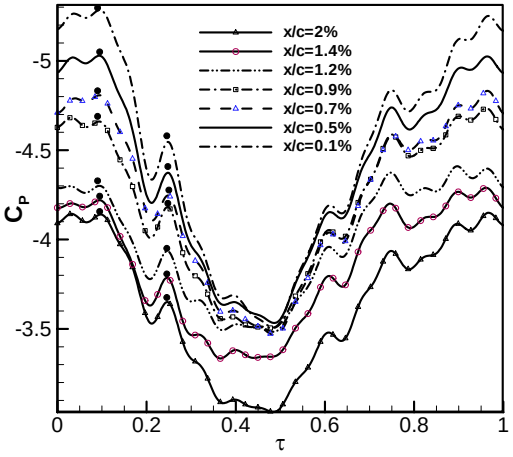

c) upper surface, near leading edge, k=0.045

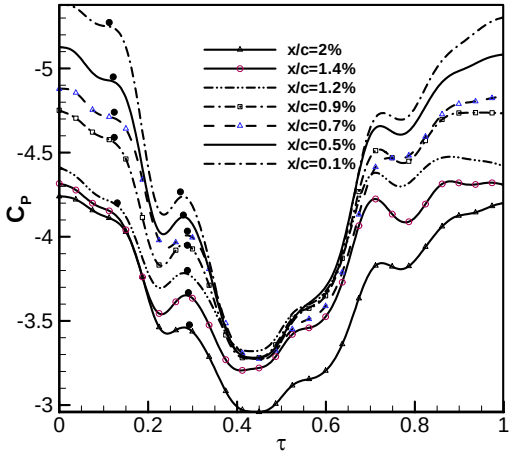

d) upper surface, near leading edge, k=0.06

Figure 5 Variation of the pressure coefficients with non-dimensional time, α_0=18º

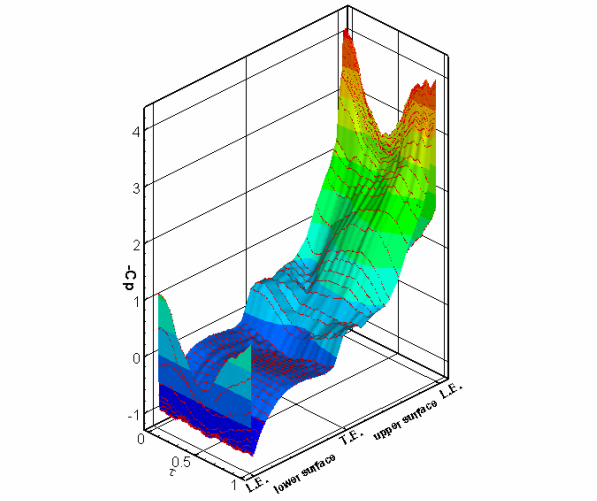

a) carpet-like graph of C_P

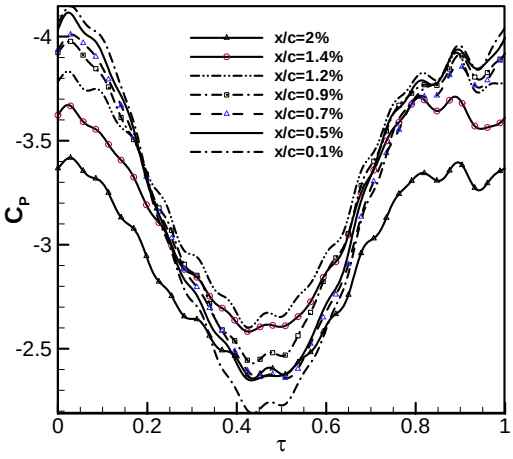

b) upper surface, near leading edge, k=0.045

Figure 6 Variation of the pressure coefficients with non-dimensional time, α_0=13º